

# Morphology and Surface Relief Structures of Asymmetric Poly(styrene-*block*-ferrocenylsilane) Thin Films

Rob G. H. Lammertink, Mark A. Hempenius, and G. Julius Vancso\*

Materials Science and Technology of Polymers, MESA+ Research Institute, University of Twente, P.O. Box 217, 7500 AE Enschede, The Netherlands

Kwanwoo Shin, Miriam H. Rafailovich, and Jonathan Sokolov

Department of Materials Science and Engineering, State University of New York at Stony Brook, New York 11794-2275

Received March 29, 2000; Revised Manuscript Received October 30, 2000

**ABSTRACT:** Thin films of an asymmetric styrene-*block*-ferrocenyldimethylsilane copolymer were studied on solid silicon substrates as well as free-standing. In the bulk the diblock forms poly(ferrocenylsilane) cylinders in a poly(styrene) matrix. The thin films were analyzed by a variety of techniques including atomic force microscopy (AFM), transmission electron microscopy (TEM), X-ray reflectivity, secondary ion mass spectrometry (SIMS), and optical microscopy. From X-ray reflectivity measurements it was concluded that both blocks were present at the substrate, whereas poly(styrene) wetted the free surface. The formation of islands and holes was observed by optical microscopy and AFM, as a result of a mismatch between the film thickness and the equilibrium spacing between layers of cylinders. Upon longer annealing of the films, the islands disappeared due to a change of the internal morphology of the thin film. After selective removal of the organic matrix by means of oxygen reactive ion etching, the phase-separated structure could be visualized by AFM. The morphology of the films altered upon annealing from an in-plane cylindrical to a hexagonal morphology. The structure in free-standing films could be analyzed by TEM. After annealing, both types of orientations of cylinders (parallel and perpendicular with respect to the surface) were found to be stable.

## Introduction

In thick block copolymer films, the mismatch between the film thickness and the bulk lattice period can be distributed over many layers. As the film thickness is decreased to a value equal to a few domain periods, the frustration due to the mismatch becomes more significant. Such thin films of block copolymers have received much attention in the past decade. To release the frustration in these films, changes in morphology have been reported for lamellar systems, i.e., symmetric block copolymers. The morphology change with decreasing thickness has been observed to depend on the specific interactions that the corresponding blocks have with their interfaces (either a free surface or a substrate). Three different situations can be distinguished: confined (between two substrates), pseudo-confined (on a substrate), and free-standing thin films (no substrate).

External interfaces influence the nature of ordering in block copolymers. Generally, a preferential affinity of one of the blocks for an interface causes the block to preferentially wet one interface. This results, for symmetric blocks, in the ordering of the lamellae parallel to this interface. A block copolymer between two confining interfaces becomes frustrated if the confined thickness is incommensurate with the natural spacing of the lamellae. As a result, these films show different periods in films compared to the bulk.<sup>1–3</sup> However, there is a limit to the extent of distortion within the lamellae. Sometimes, even perpendicularly oriented structures have been observed.<sup>4</sup> In such structures, both blocks are

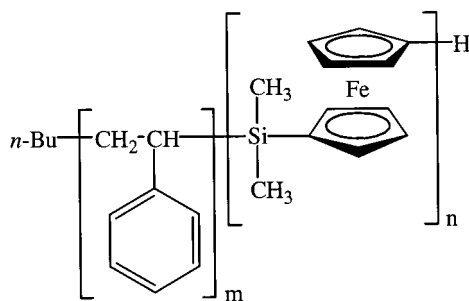
present at the interface. Theoretical predictions<sup>5–7</sup> and simulations<sup>8</sup> have supported such observations.

In pseudo-confined films, specific surface segregation results in parallel orientation of the domains with respect to the substrate. The frustration due to the mismatch between initial film thickness and bulk domain period can be released by the formation of islands, i.e., surface relief structures.<sup>9</sup> Block selective segregation at the substrate will occur when the wetting component provides the lowest interfacial tension or exhibits a specific affinity for the substrate. This results in so-called substrate-induced ordering,<sup>10</sup> which may even be present at temperatures above the bulk order–disorder temperature. The surface segregation in symmetric block copolymers is believed to be governed by enthalpic factors and can be tuned to obtain certain specificity for one block or make it neutral to both blocks.<sup>11</sup> However, if the enthalpic driving force is absent, the surface segregation can be entropy-driven, resulting in surface segregation of the more flexible chain.<sup>12,13</sup> The growth of surface relief structures has been studied in detail.<sup>14</sup>

Substrate-free block copolymer films allow one to study the thin film morphology with a noninteracting interface. The surface tension of the corresponding blocks will then induce preferential enrichment of the surface by the block with the lowest surface tension.<sup>15</sup> Such effects of interfaces on the thin film morphology have been studied for symmetric block copolymer films.<sup>16</sup>

Theoretical studies on the morphology in thin asymmetric block copolymer films also indicate interesting phenomena. In a very recent paper, a dynamic density functional theory (DDFT) was used to simulate microphases in an asymmetric block copolymer confined in a

\* Corresponding author.

**Scheme 1. Chemical Structure of the Styrene-*block*-ferrocenyldimethylsilane Copolymer****PS-*b*-PFS : SF**

thin film.<sup>17</sup> Both the film thickness and the polymer–substrate interactions influence the morphologies in the corresponding thin films. Parallel morphologies were dominant if one of the blocks had a preference for both substrates. At certain thicknesses, however, perpendicular orientation of cylinders was observed. Some noncylindrical morphologies, like parallel lamellae and perforated lamellae, have been predicted as well. Another study concluded that a lamellar region can be formed at the substrate if the affinity difference for the substrate of the two blocks is larger than some critical value.<sup>18</sup> Interacting walls do possess a profound influence on domain formation in thin films.<sup>19</sup> Suh et al.<sup>20</sup> found theoretically that cylinders in triblock and diblock copolymers could orient parallel or perpendicular in confined geometries, depending on the film thickness and interfacial energies.

Asymmetry in block copolymer composition results in interesting phenomena for thin film morphology when compared to symmetric cases.<sup>21</sup> This is easy to envisage, if one considers the case where the minority component wants to preferentially enrich the substrate surface. Even if the surface enriching block is present in the minority phase, a continuous wetting layer of that phase can still be present at the surface. Such a wetting layer can alter the near surface morphology.<sup>22,23</sup> Layers of microdomains, cylinders, or spheres oriented parallel to interfaces in asymmetric block copolymer films have been reported.<sup>24,25</sup> In the case of cylindrical domains, the domains would lie parallel, but transversely shifted, to the domains of the adjacent layer.

This paper describes the thin film morphology of an asymmetric diblock copolymer, poly(styrene-*block*-ferrocenyldimethylsilane) as illustrated in Scheme 1.<sup>26</sup> The polymer studied is a SF 27/12, which represents a 27 000 g/mol polystyrene-*b*-12 000 g/mol polyferrocenyldimethylsilane diblock. The block copolymer contains 27 vol % of the organometallic block, and the bulk structure consists of hexagonally packed cylinders of poly(ferrocenyldimethylsilane) in a poly(styrene) matrix.<sup>27</sup> Thin films were studied on silicon substrates (pseudo-confined) as well as without any substrate (free-standing). Diblock film systems are potentially very interesting if one can use them to obtain laterally structured surfaces. Such films have been recently used in “maskless” lithography applications as templates.<sup>28,29</sup> Particularly, the use of ferrocenyldimethylsilane-containing block copolymers can be employed in single step reactive ion etching processes, due to the remarkable etching barrier properties of the organometallic domains.<sup>30,31</sup>

**Experimental Section**

*N,N,N,N*-Tetramethylethylenediamine (TMEDA), ferrocene, styrene, *n*-butyllithium (1.6 M in hexanes), dibutylmagnesium (1.0 M in heptane), and dichlorodimethylsilane were obtained from Aldrich. All solvents were obtained from Merck.

TMEDA was distilled from sodium, heptane was distilled from calcium hydride, and ferrocene was Soxhlet extracted with cyclohexane prior to use. 1,1'-Dimethylsilylferrocenophane was prepared as described earlier<sup>30</sup> and purified by sequential dissolution in heptane followed by vacuum sublimation. Styrene/ethylbenzene (~10 wt % solution) was dried on dibutylmagnesium and distilled under vacuum. *n*-Butyllithium was diluted to approximately 0.2 M with heptane that was dried over *n*-butyllithium and distilled under vacuum. Tetrahydrofuran (THF) was dried over *n*-butyllithium at 0 °C and distilled under vacuum.

A poly(styrene-*block*-ferrocenyldimethylsilane) copolymer (SF, Scheme 1) was synthesized by sequential anionic polymerization carried out in an Mbraun glovebox purged with prepurified nitrogen. Polymerization of styrene in ethylbenzene (~10 wt %) was initiated by *n*-butyllithium and allowed to proceed for 5 h. After the styrene block formation had been completed, 1,1'-dimethylsilylferrocenophane was added to the solution and stirred for 5 min. Since 1,1'-dimethylsilylferrocenophane does not polymerize in ethylbenzene, THF was added to the mixture, allowing for the formation of the organometallic block. This method prevented reaction of the living polystyryl chains with THF that is known to occur at ambient temperatures. After 2 h, the living chains were terminated by adding a few drops of degassed methanol. The polymer was precipitated in methanol and dried under vacuum.

GPC measurements were carried out in THF using microstyragel columns with pore sizes of 10<sup>5</sup>, 10<sup>4</sup>, 10<sup>3</sup>, and 10<sup>6</sup> Å (Waters). The instrument was equipped with a dual detection system consisting of a differential refractometer (Waters model 410) and a differential viscometer (Viskotec model H502). Block ratios were calculated from <sup>1</sup>H NMR peak integrals. <sup>1</sup>H NMR spectra were recorded in deuterated chloroform at 250.1 MHz using a Bruker AC 250 spectrometer. The density of poly(ferrocenyldimethylsilane), 1.26 g/cm<sup>3</sup>, was obtained by means of a pycnometer.

Thin films were prepared by spin-coating on silicon wafers from toluene solutions. Film thickness could be controlled by varying the spinning speed and concentration of the copolymer solution. The film thickness was measured by ellipsometry prior to annealing. The films were annealed under vacuum at 150–160 °C. Poly(ferrocenyldimethylsilane) has a glass transition temperature of ca. 33 °C and an equilibrium melting temperature of 143 °C.<sup>32</sup>

An Olympus BX-60F3 optical microscope was employed under reflection conditions to obtain interference colors from the white light source. Nomarski interferential contrast was obtained when working in the polarizing mode.

The organic poly(styrene) matrix could be selectively removed by means of oxygen reactive ion etching. Oxygen reactive ion etching (O<sub>2</sub>-RIE) experiments were carried out in an Elektrotech PF 340 apparatus. The pressure inside the etching chamber was 10 mTorr, the substrate temperature was set at 10 °C, and an oxygen flow rate of 20 cm<sup>3</sup>/min was maintained. The power was set at 75 W. Etching times of only 10 s were found to be enough to expose the organometallic domains, so they could be visualized by AFM.

The morphology of unetched and etched films was studied by atomic force microscopy (AFM) operating in the tapping mode. AFM experiments were performed using a NanoScope III A instrument (Digital Instruments) utilizing NanoSensors tapping tips. Etched films could be studied best at low amplitudes of oscillation at free vibration (*A*<sub>0</sub> = 1.0 V) and relatively high operating set point ratios (*A*<sub>sp</sub>/*A*<sub>0</sub> ~ 0.9). The use of a lower set point ratio, or high amplitudes at free vibration, frequently resulted in severe tip damaging. Height images were recorded at a scanning rate of 1 Hz.

Free-standing films were prepared by spin-coating an approximately 70 nm thin film onto a silicon wafer. The film was

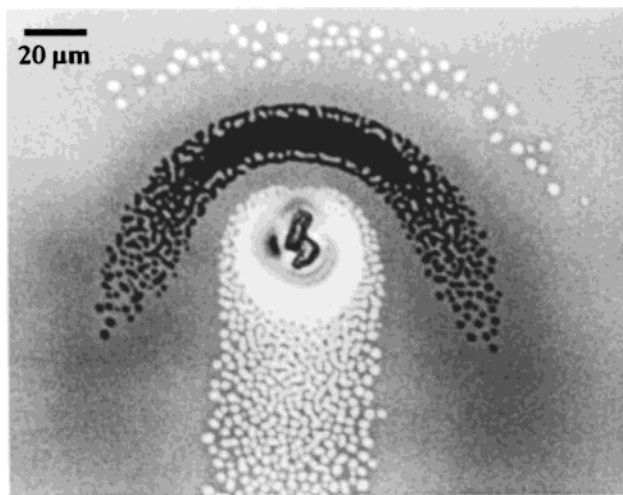


**Figure 1.** Optical interference micrograph of the area around a dust particle in a 40 nm thick SF 27/12 film, after annealing for 24 h at 150 °C. The gray area represents the 40 nm thick film, whereas the lighter and darker areas correspond to film thicknesses that are one period layer thinner and thicker, respectively.

floated off on a water bath and picked up with a copper TEM grid. The films were then annealed under vacuum at 150 °C.

Transmission electron microscopy (TEM) images of free-standing films were obtained using a JEOL 200 CX and Philips CM30 electron microscope. The sample holders in these setups could be tilted. No staining was required for TEM, due to the larger electron density of the organometallic phase.

X-ray reflectivity measurements were carried out at the beamline X10B of the National Synchrotron Light Source at Brookhaven National Laboratory using a wavelength of 1.127 Å. Analysis of the reflectivity data was performed using a new Fourier method, which allows one to evaluate even low contrast layered systems.<sup>41</sup>

Depth profiling was performed on a SIMS Atomika instrument with an Ar beam at 2 keV rastered over a  $1 \times 1$  mm<sup>2</sup> spot. The samples were covered by a sacrificial thin film of deuterated poly(styrene) by floating it onto the diblock film. This procedure ensured that steady-state sputtering conditions were achieved before the sputtering crater reached the original copolymer surface. Positive Fe and Si and negative deuterium and carbon were monitored as a function of sputtering time. The thickness of the film was measured with ellipsometry, and the depth scale was obtained by dividing the carbon trace by the total thickness.

## Results and Discussion

**Thin Films on Silicon Substrates.** The block copolymer used for the thin film study, described in this paragraph, possessed a cylindrical morphology in the bulk.<sup>27</sup> The specimen, denoted by SF 27/12, is a 27 000 g/mol polystyrene-*b*-12 000 g/mol polyferrocenyldisilane diblock.

After annealing SF 27/12 for 24 h at 150 °C on a silicon substrate, the film forms islands and holes for film thicknesses that are incommensurate with the domain spacing. As is displayed in Figure 1, gradual film thickness variations become "quantized" at specific thicknesses after annealing. The formation of plateaus is indicative of an oriented structure, with the nano-domains lying parallel to the film substrate and surface.

The formation of islands and holes can be observed for films with an initial thickness that is incommensurate with the equilibrium domain spacing. The diblock considered forms a cylindrical phase in the bulk with a lattice spacing of approximately 26 nm.<sup>27</sup> De-

pending on which of the phases will be present at the surface and/or the substrate, islands and holes at specific thicknesses are formed. It was shown in the literature that even when the minority phase has a preference for the substrate, it might still wet the substrate and thereby form a lamellar layer at this substrate.

Contact angle measurements performed on the corresponding homopolymers could not distinguish between poly(styrene) and poly(ferrocenyldimethylsilane).<sup>33</sup> Thus, the obviously low difference in surface energy results in a small driving force for one of the phases to wet the surface. From XPS measurements, however, it was determined that poly(styrene) is covering the surface of thin PS-*b*-PFS films after annealing.

Initially flat films can form islands or holes after annealing if the film thickness is incommensurate with the domain spacing. At a film thickness of approximately 52 nm, which is about equal to 2 times the lattice spacing, the film forms an almost bicontinuous islands and holes structure after annealing for 2 days at 160 °C (see Figure 2). The height of the terraces, however, is similar to the lattice spacing of the diblock copolymer. So, from the corresponding AFM image, we can already conclude that the majority phase, poly(styrene), is *not* present at *both* the surface and the substrate. If poly(styrene) was present at both the substrate and the surface, such a structure would exactly fill a 52 nm thin film with two layers of cylinders (since each layer is about 26 nm thick). XPS measurements indicated that poly(styrene) wets the free surface of the block copolymer film. Therefore, the organometallic block is probably present at the substrate. From theoretical studies it was already shown that a lamellar region might be present at the substrate, if the difference between the affinity of the two phases for the substrate is large enough. Otherwise, both phases might be present at the substrate.<sup>18</sup>

The area occupied by islands is approximately 50% of the total film surface as displayed in Figure 2. Together with an island height of about 26 nm (equal to the bulk lattice spacing), this implies that the thickness of the film in a valley is ca. 39 nm. Indeed, a film with an initial thickness of 39 nm does not form any islands but remains continuous after annealing, implying that a film thickness of 39 nm is commensurate with the domain spacing. Accordingly, since the commensurate film thickness approximately equals  $(n + 1/2)L_0$ , in which  $n$  is an integer and  $L_0$  is the bulk period, this suggests asymmetric surface boundary conditions for this block copolymer system on silicon substrates.

To obtain information about the internal microstructure of the thin diblock film, we have to "zoom in" in order to visualize the domains. Typically, transmission electron microscopy (TEM) is used to study phase separation in block copolymer systems. For the thin films described in this study, however, the silicon substrate does not allow the use of TEM since it is not transparent for electrons. Another possibility for thin film studies is the use of atomic force microscopy (AFM). The difference in mechanical response of the different domains allows one to visualize these domains by AFM tapping mode phase imaging. The use of AFM in imaging block copolymer thin films has proven to be a successful tool to study the lateral morphology on a nanometer level.<sup>34</sup> However, the interpretation of phase

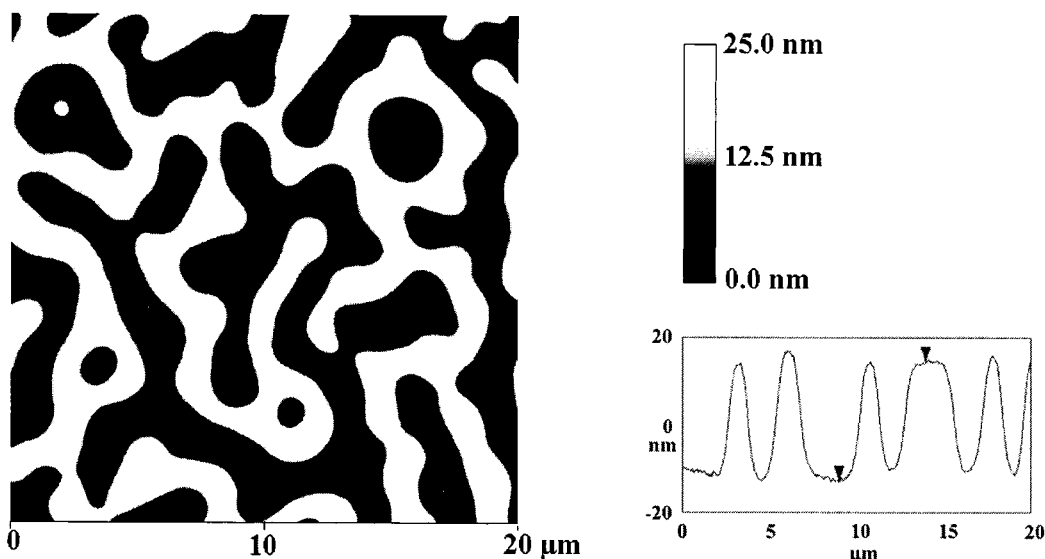


**Figure 2.** AFM height image of an annealed 52 nm thin film of SF 27/12 on a silicon substrate. The terraces are approximately 25–27 nm higher compared to the valleys, as can be observed in the line scan on the right.

contrast is not straightforward, and care should be taken in identifying the phases by their relative contrast in height and phase modes since the contrast is sensitive to changes in the operation conditions of the microscope.<sup>35,36</sup>

The applicability of AFM phase imaging to study the phase-separated morphology of thin poly(styrene-*block*-ferrocenylsilane) copolymer films was found to be limited. Because of the surface coverage of the poly(styrene) phase, the underlying structure could not be visualized directly. If a soft phase would form the matrix of the film, the AFM tip could penetrate through the covering layer and image the underlying structure, as demonstrated in a previous study on poly(isoprene-*block*-ferrocenylsilane) thin films.<sup>37</sup> This was not possible in our case due to the glassy nature of PS.

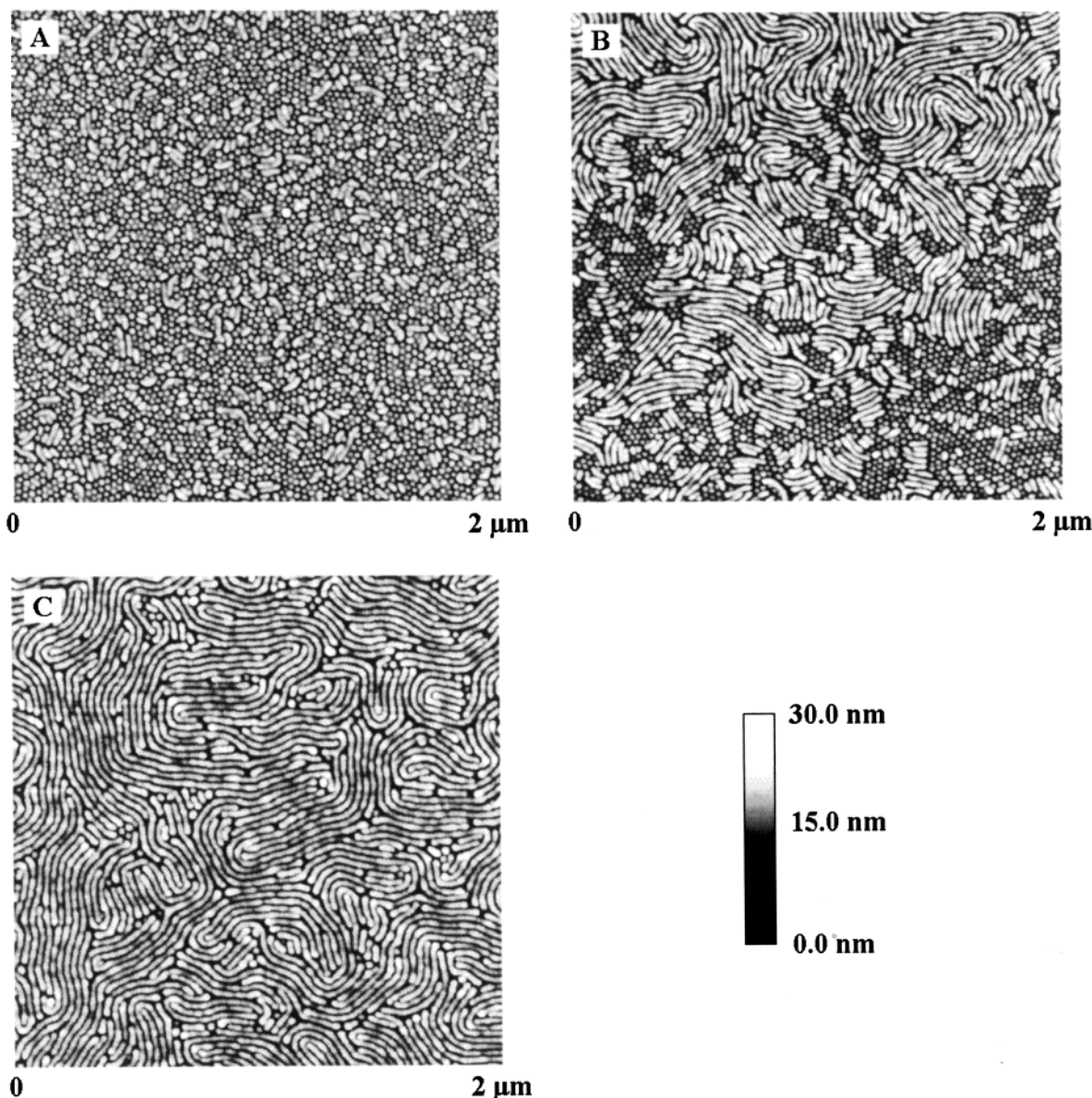
To overcome this problem, we selectively removed the organic poly(styrene) matrix by means of oxygen reactive ion etching (O<sub>2</sub>-RIE). In oxygen plasma, organic substances are quickly removed. The organometallic polymer forms a thin protective oxide layer upon exposure to an oxygen plasma. The removal of the organometallic component is then slowed due to the competition between the oxide formation by the plasma and the ion sputtering effect. As a result, a high etching rate difference, up to 50:1, can be obtained between the organic and organometallic phases, and the organic phase can be selectively removed.<sup>30</sup>

Figure 3 displays the AFM images of annealed SF 27/12 thin films of different thicknesses, after the selective removal of the organic phase by means of O<sub>2</sub>-RIE. A full layer of in-plane cylinders can be observed for a 40 nm thick film (Figure 3C). The film thickness is then about equal to the thickness of the film in the valleys from Figure 2. Probably the film consists of a single layer of cylinders on top of a thin lamellar wetting layer at the substrate. If the initial thickness is lower than approximately 40 nm, the single layer of cylinders cannot be completely formed. As can be observed in Figure 3B for a film thickness of 35 nm, in such cases areas are formed where a hexagonal structure is present. This becomes even more pronounced at a film thickness of 30 nm (Figure 3A). Thus, the mismatch between the initial film thickness and the equilibrium lattice spacing

can be balanced by a change in morphology or domain orientation.<sup>38</sup> However, the height of the domains in the areas where the hexagonal structure is present seems to be less compared to the height of the in-plane cylinders. This suggests that the hexagonal structure does *not* consist of perpendicularly oriented cylinders.

From the Fourier transforms of the images in Figure 3, the lattice spacing could be determined. The spacing was found to be 26 nm for image A, 27 nm for image B, and 29 nm for image C. In the bulk, the cylinders have a lattice spacing of 26 nm, which results in a cylinder-to-cylinder distance of about 30 nm. The spacing from the Fourier transform of image A can be directly related to the spacing from SAXS measurements performed on bulk samples, since both possess a hexagonal structure. Furthermore, the spacing from image C is in quite good agreement with the bulk distance between cylinders. Since image B consists of a mixed morphology, the average spacing from the Fourier transform has an intermediate value.

Provided that the thickness of film is not commensurate with the domain period, islands or holes are formed. This is illustrated in Figure 4, for a 47 nm thin film that was annealed at 150 °C for different times. After 24 h, the film is still quite smooth, and the morphology consists of cylinders oriented parallel to the surface. Near the slightly elevated structures, some defects in the morphology ("dots") are frequently observed. A well-developed island can be observed in Figure 4B, after annealing for 48 h. Within the island and the valleys, the cylinders are oriented parallel to the surface, whereas a sort of corona is present around the island that displays a hexagonal, dotlike structure. Defect structures near island edges have been previously observed. For example, the steps between terraces in symmetric block copolymer films were found to consist of perpendicularly oriented lamellae.<sup>10h</sup> In asymmetric diblock films, forming a cylindrical morphology, edge defects were interpreted as a layer of spheres above a perforated lamella, with the spheres positioned above the perforations.<sup>39</sup> Such domain edge structures play an important role during the growth and coarsening of islands. Surprisingly, after further annealing, the islands slowly disappeared, and the complete film pos-



**Figure 3.** AFM height images, taken in tapping mode, of thin SF 27/12 films of different thicknesses after annealing for less than 2 days at 150 °C. The organic matrix phase was selectively removed prior to AFM imaging by means of O<sub>2</sub>-RIE treatment for 10 s, leaving the organometallic structure behind. (A) 30 nm film thickness, (B) 35 nm film thickness, (C) 40 nm film thickness.

sessed a hexagonal structure (Figure 4C). So, after annealing for more than 3–4 days, the surface of the film became smooth again, with a uniform thickness that was incommensurate with the lattice period. Such a process can be explained by a change in domain orientation, but also by a change in the near interface morphology.<sup>18</sup>

Fourier transforms of the AFM images were determined also for the features exhibited in Figure 4 to estimate average repeat periods. Image A and B have spacings according to Fourier analysis, of approximately 28 nm, which is close to the value of 30 nm corresponding to the bulk cylinder-to-cylinder distance. Perhaps the cylinders are slightly compressed for images A and B, since the film thickness is not commensurate with the domain spacing; i.e., the film is too thick. The Fourier transform of image C indicated a spacing of about 35 nm, which results in a domain-to-domain distance of approximately 40 nm for a hexagonal structure. The large discrepancy between the domain-to-domain distance in the bulk (30 nm) compared to the

thin film (40 nm) suggests that the structure in image C is *not* a result of perpendicularly oriented cylinders. Spheres on a bcc lattice have approximately the same spacing for their (110) planes as the spacing of (100) planes in a hexagonal cylindrical morphology.<sup>40</sup> Thus, a transition from cylinders to spheres near the film surface cannot account for the large deviation in the period spacing either.

To gain information about the in-depth morphology of the thin diblock films, X-ray reflectivity and secondary ion mass spectroscopy (SIMS) measurements were performed. A layered morphology, with its layers parallel to the substrate and surface, gives rise to changes in the density perpendicular to the film. Such changes can be measured by X-ray reflectivity experiments.

From secondary ion mass spectrometry (SIMS) a first guess about the internal film structure in the perpendicular direction can be obtained. The depth profile displays an oscillating signal for iron and silicon, which are present in the organometallic block. At the substrate the silicon signal shows a sharp increase due to the

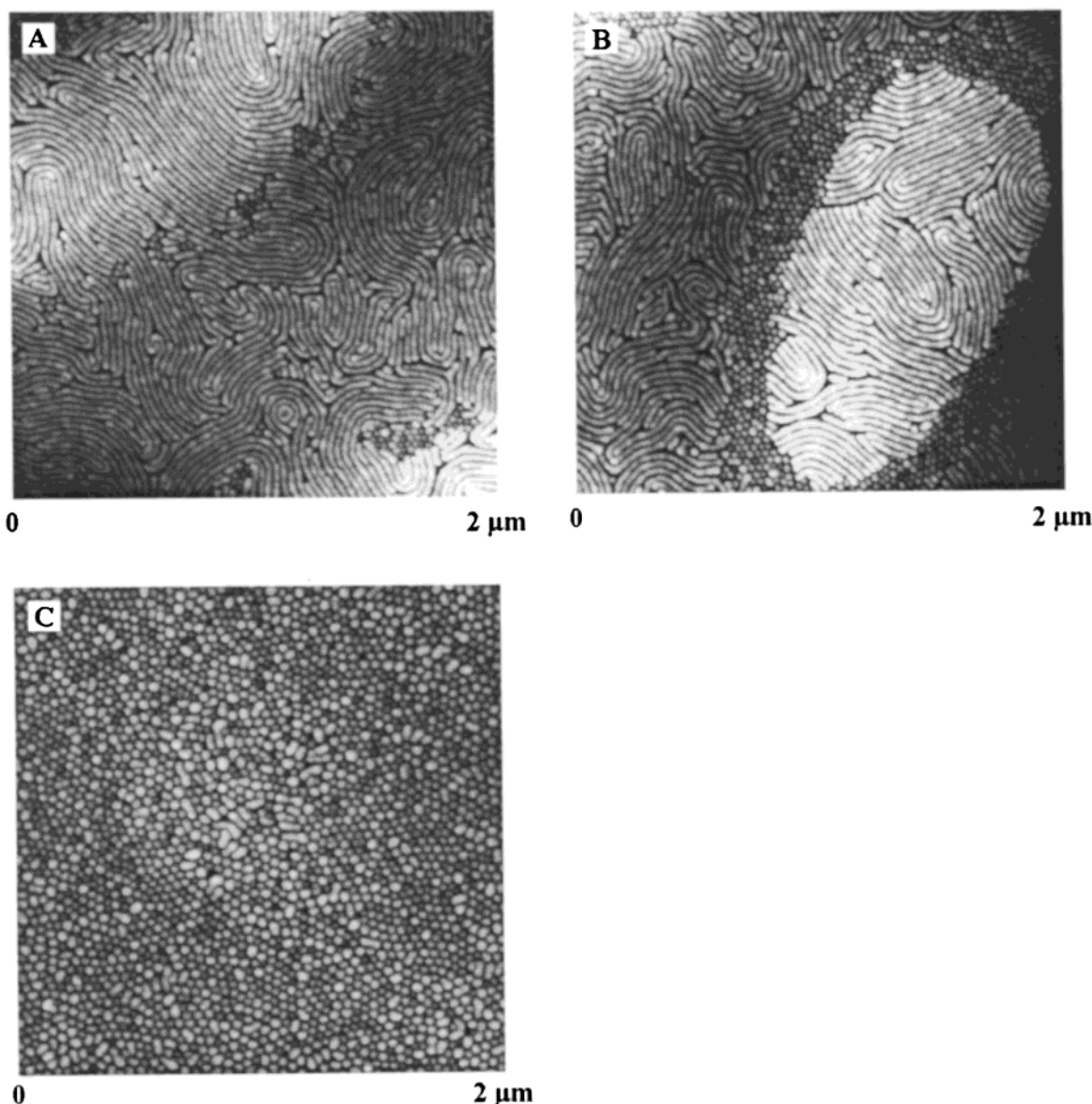


**Figure 4.** AFM height images of a 47 nm thin SF 27/12 film after annealing at 150 °C for different times: (A) 24 h, (B) 48 h, (C) 96 h.

substrate. The SIMS results were converted to volume fraction of PFS as a function of film depth and are displayed in Figure 5. The volume fraction of PFS oscillates as a result of the alignment of the domains parallel to the substrate. The poly(ferrocenylsilane) block is present at the silicon substrate. The volume fraction of PFS at the silicon substrate is comparable to the bulk volume fraction of the diblock (0.27) whereas the volume fraction in the layers, which are oriented parallel to the substrate, exceeds the value of the bulk volume fraction. The distance between the two layers is approximately 20 nm, which is less than the period observed in the bulk sample (26 nm).

The information obtained from the SIMS experiments can be used as a first approximation for the calculation of a density profile from X-ray reflectivity measurements. These measurements were performed on the same films as used for the SIMS experiments (Figure 6). In general, the electron density contrast between different phases in block copolymer thin films is quite low, and therefore neutron scattering is usually used to investigate such polymer layers. However, deuteria-

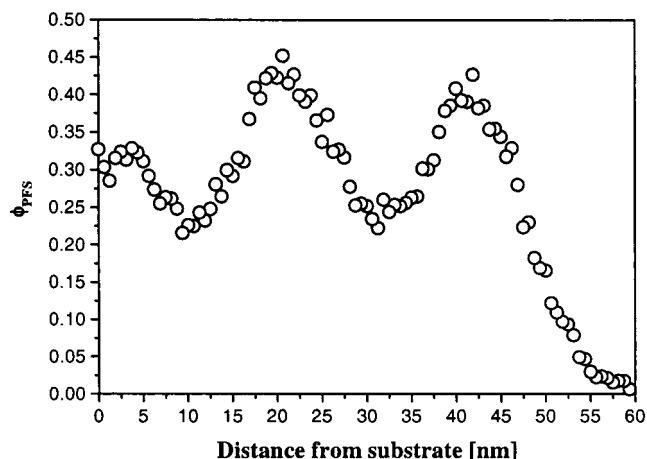


**Figure 5.** Volume fraction of PFS plotted against the distance from the substrate, obtained from the SIMS spectrum for a 50 nm thin film of SF 27/12, annealed for 20 h at 150 °C.

tion may change the phase behavior of the polymers. A novel analysis method was recently developed to obtain

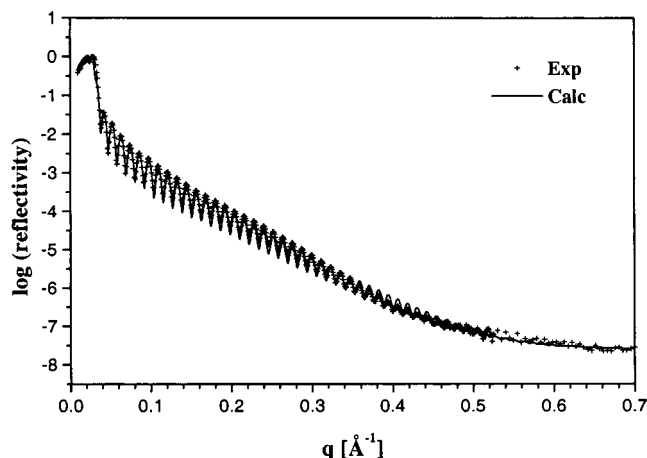


**Figure 6.** X-ray reflectivity data of a thin SF 27/12 film that was annealed for 20 h at 150 °C.

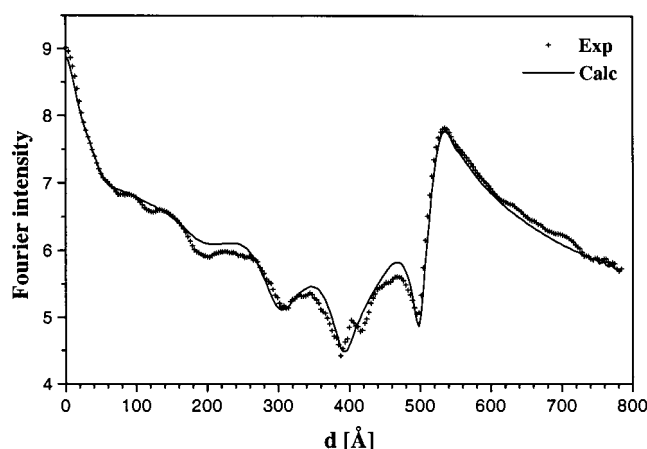


**Figure 7.** Fourier transform intensity of X-ray reflectivity curves as displayed in Figure 6.

accurate information about the density depth profile of block copolymer thin films utilizing X-rays (i.e., no deuteration is needed for this procedure).<sup>41</sup>

If one would be using the well-known Parratt algorithm to obtain the density depth profile,<sup>42</sup> only the substrate–film and film–air interface could be subtracted from these data. By using the new Fourier method,<sup>41</sup> which takes into account different limits of integration in  $q$ -space, the interfacial parameters can be determined with high accuracy although the difference in the electron density (the contrast) of the two phases may still be very small.

In the Fourier intensity profile, several small peaks are visible besides the large peak at  $d = 500$  Å in Figure 7. These small peaks contain information about the low contrast interface. The simulated reflectivity and Fourier transformed intensities were calculated from a refractive index depth profile. The initial guess for the iteration process that leads to the final profile was taken from the SIMS data.

The refractive index (related to the electron density) depth profile is shown in Figure 8. In this figure, the substrate is situated near  $z = 0$ , and the film has a total thickness of about 50 nm. From this profile, it can be concluded that the organometallic ferrocenylsilane phase is present at the substrate, whereas the organic styrene phase enriches the surface (as was also shown by XPS measurements). This is in full agreement with the observations from AFM, which indicated so-called asym-

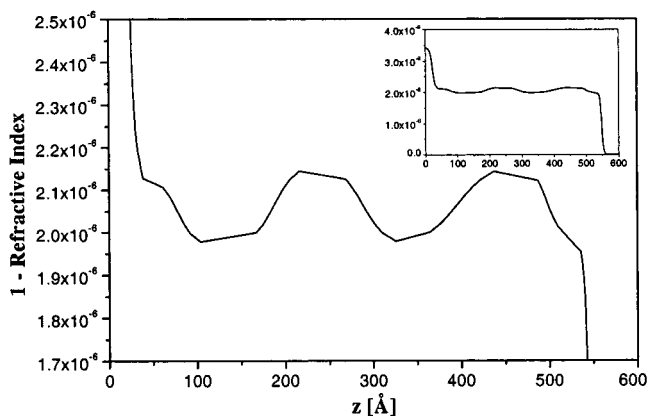


**Figure 8.** Simulated density depth profile (expressed in terms of refractive index variation), as obtained from X-ray reflectivity data, using the Fourier method from ref 41. The inset displays the entire profile.

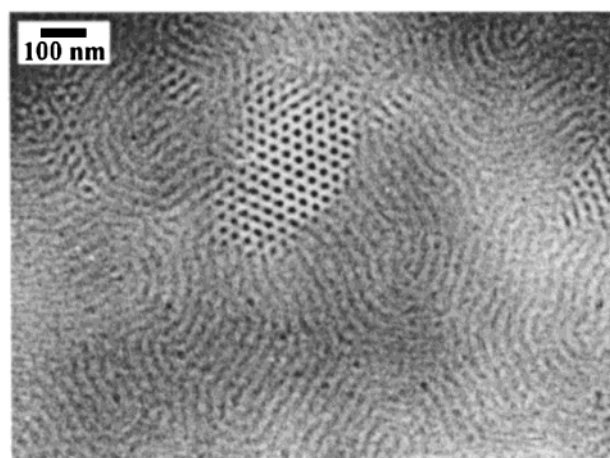


**Figure 9.** TEM image of a free-standing film of SF 27/12, after annealing for 24 h at 150 °C. The morphology consists of cylinders of poly(ferrocenylsilane) (dark) in a poly(styrene) matrix (bright). A few small areas contain perpendicular oriented cylinders.

metric wetting. However, a wetting layer of the organometallic phase at the substrate would result in a relatively large volume fraction PFS (close to 1). SIMS and X-ray reflectivity data clearly indicated that this is not the case. Moreover, the results suggested that both phases can be found near the substrate. Obviously, the affinity for one of the two phases is not large enough to induce the lamellar ordering at the substrate, but rather both blocks are in contact with the substrate.<sup>18</sup>

Interestingly, the thickness of the film is comparable to the thickness of the film displayed in Figure 2. So, if a film of this thickness (approximately 50 nm) is annealed for only 1 day, the film remains flat and the internal structure evolves. The spacing between the two layers in the density profile is approximately 22 nm. This implies that the morphology of the film is frustrated, since the equilibrium lattice spacing in the bulk is approximately 26 nm. After longer annealing, for several days, the film becomes more and more unsatisfied with its initial thickness, and surface relief structures are formed.

Upon annealing block copolymer thin films, phase separation starts first with the orientation of the cylinders parallel to the surface. If the film thickness is incommensurate with the equilibrium layer thickness, islands or holes are developing.

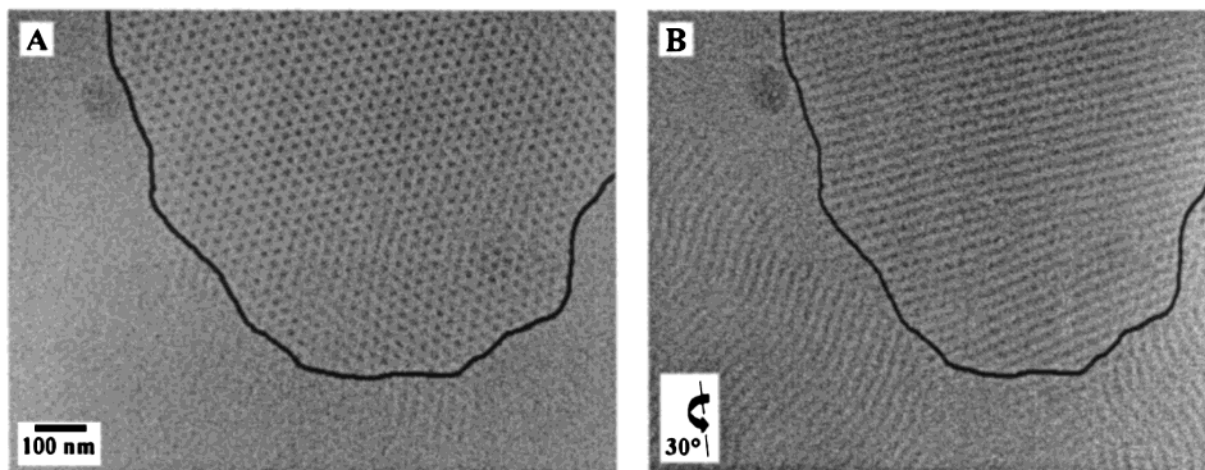


**Figure 10.** TEM micrographs of a free-standing SF 27/12 film. Image A was taken without any tilt, showing a grain boundary. Within this grain the domains are hexagonally arranged. Image B was taken at 30° tilt, illustrating that the hexagonally packed domains are perpendicularly oriented cylinders. Furthermore, the parallel oriented cylinders become visible when the sample is tilted.

**Free-Standing Diblock Copolymer Films.** Diblock copolymer thin films can be annealed without the presence of a substrate. To explore the morphology of such films, a thin film was spin-coated on a silicon wafer, after which the film was removed by using a lift-off technique in a water bath. The floating copolymer film was picked up with a TEM copper grid. During subsequent annealing the film did not experience contact with any substrate.

In Figure 9, a TEM image of a free-standing film of SF 27/12 is displayed. The sample was annealed for 24 h at 150 °C. The majority of the film consists of cylinders that are oriented parallel to the surface, since the majority component, poly(styrene), wets both free surfaces (symmetric wetting). A few small areas were observed where the organometallic cylinders have a perpendicular orientation.

The orientation of the cylinders within the film can be nicely illustrated by tilting the specimen in the electron microscope. This is displayed in Figure 10. The film displayed in this figure was annealed for 4 days, which resulted in an increase of the areas with a perpendicular orientation.

Upon longer annealing times, the areas with perpendicularly oriented cylinders were observed to become larger. Perpendicularly oriented cylinders have been observed before, but they were presumably a result of the film preparation, i.e., quick solvent evaporation.<sup>43</sup> In other words, perpendicularly oriented cylinders were found to be metastable thus far, since the higher surface free energy block would also be present at the surface.<sup>44</sup> The perpendicular orientation in free-standing films of poly(styrene-*block*-ferrocenyldimethylsilane) however seems to be a stable morphology.

An explanation for the perpendicular orientation may be that the difference in surface free energy between the two phases is small enough to allow both blocks to be present at the surface. In doing so, the frustration within the film due to the mismatch between the film thickness and the domain period can be released. As earlier mentioned, from contact angle measurements the surface energies of poly(styrene) and poly(ferrocenyldimethylsilane) were found to be approximately equal within the accuracy of the measurements. In a theoretical study, it was concluded that if the difference

between tendency for surface segregation is below a certain value, perpendicular orientation could be favorable, since it releases the frustration by allowing both blocks at the same interface.<sup>20</sup> For a perpendicular orientation of cylinders, the equilibrium period of the block copolymer system can be realized, whereas this is not possible in the parallel morphology without the formation of islands or holes.

## Conclusions

Thin film morphologies of asymmetric styrene-*block*-ferrocenyldimethylsilane copolymers were studied. The microdomain structure could be visualized by AFM height imaging after selective removal of the organic matrix by means of oxygen reactive ion etching. The thin film morphology after annealing consisted of cylinders that are oriented parallel to the surface. Upon annealing, the films formed surface relief structures if the film thickness was incommensurate with the equilibrium spacing period. These observations are all in agreement with previous studies on asymmetric block copolymer thin films and are a result of the surface boundary conditions of these block copolymers on silicon substrates. From SIMS and X-ray reflectivity measurements, it was concluded that both poly(styrene) and poly(ferrocenylsilane) are present at the silicon substrate whereas poly(styrene) preferentially wets the free surface. The preferential aggregation at the free surface induces parallel orientation of the microdomains with respect to the interface. However, after longer annealing periods, usually more than 4 days, the surface relief structures disappeared accompanied by a change of the microstructure, i.e., a change in domain orientation or a morphological transition.

For free-standing films both orientations of the cylinders were found to be present in annealed samples. The perpendicular orientation of cylinders seems to be stable as well, since the amount of perpendicularly oriented cylinders is increasing in time during annealing. The perpendicular orientation allowed for the film thickness to become incommensurate with the equilibrium spacing while maintaining the equilibrium period, so the stress could be relieved without the formation of surface relief structures (islands or holes). These results are also relevant in view of the unique potential of these

organic–organometallic block copolymers in applications as lithographic masks for reactive ion etching.

## References and Notes

- (1) Lambooy, P.; Russell, T. P.; Kellogg, G. J.; Mayes, A. M.; Gallagher, P. D.; Satija, S. K. *Phys. Rev. Lett.* **1994**, *72*, 2899.
- (2) Koneripalli, N.; Singh, N.; Levicky, R.; Bates, F. S.; Gallagher, P. D.; Satija, S. K. *Macromolecules* **1995**, *28*, 2897.
- (3) Koneripalli, N.; Levicky, R.; Bates, F. S.; Ankner, J.; Kaiser, H.; Satija, S. K. *Langmuir* **1996**, *12*, 6681.
- (4) Kellogg, G. J.; Walton, D. G.; Mayes, A. M.; Lambooy, P.; Russell, T. P.; Gallagher, P. D.; Satija, S. K. *Phys. Rev. Lett.* **1996**, *76*, 2503.
- (5) Walton, D. G.; Kellogg, G. J.; Mayes, A. M.; Lambooy, P.; Russell, T. P. *Macromolecules* **1994**, *27*, 6225.
- (6) Pickett, G. T.; Balazs, A. C. *Macromolecules* **1997**, *30*, 3097.
- (7) Matsen, M. W. *J. Chem. Phys.* **1997**, *106*, 7781.
- (8) (a) Kikuchi, M.; Binder, K. *Europhys. Lett.* **1993**, *21*, 427. (b) Kikuchi, M.; Binder, K. *J. Chem. Phys.* **1994**, *101*, 3367.
- (9) Coulon, G.; Ausserre, D.; Russell, T. P. *J. Phys. (Paris)* **1990**, *51*, 777.
- (10) Surface-induced ordering in thin films has been studied by several techniques, such as neutron reflectivity, secondary ion mass spectroscopy (SIMS), and transmission electron microscopy (TEM). (a) Anastasiadis, S. H.; Russell, T. P.; Satija, S. K.; Majkrzak, C. F. *Phys. Rev. Lett.* **1989**, *62*, 1852. (b) Anastasiadis, S. H.; Russell, T. P.; Satija, S. K.; Majkrzak, C. F. *J. Chem. Phys.* **1990**, *92*, 5677. (c) Menelle, A.; Russell, T. P.; Anastasiadis, S. H.; Satija, S. K.; Majkrzak, C. F. *Phys. Rev. Lett.* **1992**, *68*, 67. (d) Mayes, A. M.; Russell, T. P.; Bassereau, P.; Baker, S. M.; Smith, G. S. *Macromolecules* **1994**, *27*, 749. (e) Gadegaard, N.; Almdal, K.; Larsen, N. B.; Mortensen, K. *Appl. Surf. Sci.* **1999**, *142*, 608. A selection of papers on thin block copolymer films that have been studied by SIMS: (f) Coulon, G.; Russell, T. P.; Deline, V. R.; Green, P. F. *Macromolecules* **1989**, *22*, 2581. (g) Russell, T. P.; Coulon, G.; Deline, V. R.; Miller, D. C. *Macromolecules* **1989**, *22*, 4600. TEM can be used to elucidate the morphology within thin films: (h) Carvalho, B. L.; Thomas, E. L. *Phys. Rev. Lett.* **1994**, *73*, 3321. (i) Carvalho, B. L.; Lescanec, R. L.; Thomas, E. L. *Macromol. Symp.* **1995**, *98*, 1131. (j) Liu, Y.; Rafailovich, M. H.; Sokolov, J.; Schwarz, S. A.; Bahal, S. *Macromolecules* **1996**, *29*, 899.
- (11) (a) Mansky, P.; Russell, T. P.; Hawker, C. J.; Pitsikalis, M.; Mays, J. *Macromolecules* **1997**, *30*, 6810. (b) Mansky, P.; Russell, T. P.; Hawker, C. J.; Mays, J.; Cook, D. C.; Satija, S. K. *Phys. Rev. Lett.* **1997**, *79*, 237.
- (12) (a) Foster, M. D.; Sikka, M.; Singh, N.; Bates, F. S.; Satija, S. K.; Majkrzak, C. F. *J. Chem. Phys.* **1992**, *96*, 8605. (b) Sikka, M.; Singh, N.; Karim, A.; Bates, F. S.; Satija, S. K.; Majkrzak, C. F. *Phys. Rev. Lett.* **1993**, *70*, 307.
- (13) A theoretical analysis of blends of stiff and flexible chains agreed with the experimental observations that the surface is enriched by the more flexible chain: Frederickson, G. H.; Donley, J. P. *J. Chem. Phys.* **1992**, *97*, 8941. However, simulations have pointed out that surface segregation can be entropy driven, resulting in surface enrichment by the stiffer polymer: (a) Yethiraj, A.; Kumar, S.; Hariharan, A.; Schweizer, K. S. *J. Chem. Phys.* **1994**, *100*, 4691. (b) Kumar, S. K.; Yethiraj, A.; Schweizer, K. S.; Leermakers, F. A. M. *J. Chem. Phys.* **1995**, *103*, 10332. (c) Yethiraj, A. *Phys. Rev. Lett.* **1995**, *74*, 2018.
- (14) (a) Coulon, G.; Collin, B.; Ausserre, D.; Chatenay, D.; Russell, T. P. *J. Phys. (Paris)* **1990**, *51*, 2801. (b) Maaloum, M.; Ausserre, D.; Chatenay, D.; Coulon, G.; Gallot, Y. *Phys. Rev. Lett.* **1992**, *68*, 1575. (c) Collin, B.; Chatenay, D.; Coulon, G.; Ausserre, D.; Gallot, Y. *Macromolecules* **1992**, *25*, 1621. (d) Cai, Z.; Huang, K.; Montano, P. A.; Russell, T. P.; Bai, J. M.; Zajac, G. W. *J. Chem. Phys.* **1993**, *98*, 2376. (e) Mutter, R.; Stühn, B. *Macromolecules* **1995**, *28*, 5022. (f) Grim, P. C. M.; Nyrkova, I. A.; Semenov, A. N.; ten Brinke, G.; Hadzioannou, G. *Macromolecules* **1995**, *28*, 7501. (g) Vignaud, G.; Gibaud, A.; Grübel, G.; Joly, S.; Ausserre, D.; Legrand, J. F.; Gallot, Y. *Phys. B* **1998**, *248*, 250. (h) Heier, J.; Sivanian, E.; Kramer, E. J. *Macromolecules* **1999**, *32*, 9007.
- (15) Rastogi, A. K.; St. Pierre, L. E. *J. Colloid Interface Sci.* **1969**, *31*, 168.
- (16) Liu, Y.; Rafailovich, M. H.; Sokolov, J.; Schwarz, S. A.; Bahal, S. *Macromolecules* **1996**, *29*, 899.
- (17) Huinink, H. P.; Brokken-Zijp, J. C. M.; van Dijk, M. A.; Sevink, G. J. A. *J. Chem. Phys.* **2000**, *112*, 2452.
- (18) Turner, M. S.; Rubinstein, M.; Marques, C. M. *Macromolecules* **1994**, *27*, 4986.
- (19) Brown, G.; Chakrabarti, A. *J. Chem. Phys.* **1994**, *101*, 3310.
- (20) Suh, K. Y.; Kim, Y. S.; Lee, H. H. *J. Chem. Phys.* **1998**, *108*, 1253.
- (21) Radzilewski, L. H.; Carvalho, B. L.; Thomas, E. L. *J. Polym. Sci., Part B: Polym. Phys.* **1996**, *34*, 3081.
- (22) Yokoyama, H.; Kramer, E. J.; Rafailovich, M. H.; Sokolov, J.; Schwarz, S. A. *Macromolecules* **1998**, *31*, 8826.
- (23) Liu, Y.; Zhao, W.; Zheng, X.; King, A.; Singh, A.; Rafailovich, M. H.; Sokolov, J.; Dai, K. H.; Kramer, E. J.; Schwarz, S. A.; Gebizlioglu, O.; Sinha, S. K. *Macromolecules* **1994**, *27*, 4000.
- (24) (a) Karim, A.; Singh, N.; Sikka, M.; Bates, F. S.; Dozier, W. D.; Felcher, G. P. *J. Chem. Phys.* **1994**, *100*, 1620. (b) Henkee, C. S.; Thomas, E. L.; Fetters, L. J. *J. Mater. Sci.* **1988**, *23*, 1685.
- (25) Yokoyama, H.; Mates, T. E.; Kramer, E. J. *Macromolecules* **2000**, *33*, 1888.
- (26) For anionic polymerization of ferrocenophanes see for example: (a) Rulkens, R.; Lough, A. J.; Manners, I. *J. Am. Chem. Soc.* **1994**, *116*, 797. (b) Ni, Y. Z.; Rulkens, R.; Manners, I. *J. Am. Chem. Soc.* **1996**, *118*, 4102. For a review on poly(ferrocenylsilanes) see: (c) Manners, I. *Chem. Commun.* **1999**, 857.
- (27) Lammertink, R. G. H.; Hempenius, M. A.; Thomas, E. L.; Vancso, G. J. *J. Polym. Sci., Part B: Polym. Phys.* **1999**, *37*, 1009.
- (28) Spatz, J. P.; Sheiko, S.; Möller, M. *Adv. Mater.* **1996**, *8*, 513.
- (29) Park, M.; Harrison, C.; Chaikin, P. M.; Register, R. A.; Adamson, D. H. *Science* **1997**, *276*, 1401.
- (30) (a) Lammertink, R. G. H.; Hempenius, M. A.; van den Enk, J. E.; Chan, V. Z.-H.; Thomas, E. L.; Vancso, G. J. *Adv. Mater.* **2000**, *12*, 98. (b) Lammertink, R. G. H.; Hempenius, M. A.; Vancso, G. J.; Chan, V. Z.-H.; Thomas, E. L. Abstract ACS, *PMSE Prepr.* **1999**, *81*, 14.
- (31) Lammertink, R. G. H.; Hempenius, M. A.; Vancso, G. J. *Chem. Mater.*, in press.
- (32) Lammertink, R. G. H.; Hempenius, M. A.; Manners, I.; Vancso, G. J. *Macromolecules* **1998**, *31*, 795.
- (33) The contact angles of liquids with the poly(styrene) and poly(ferrocenylsilane) surfaces were approximately 90° for water, 55° for diiodomethane, and 78° glycerol. Using the acid–base interaction theory (van Oss, C. J.; Ju, L.; Chaudhury, M. K.; Good, R. J. *J. Colloid Interface Sci.* **1989**, *128*, 313), this resulted in a surface energy  $\gamma = 33$  mN/m.
- (34) Leclère, Ph.; Lazzaroni, R.; Brédas, J. L.; Yu, J. M.; Dubois, Ph.; Jérôme, R. *Langmuir* **1996**, *12*, 4317.
- (35) Bar, G.; Thomann, Y.; Brandsch, R.; Cantow, H.-J.; Whangbo, M.-H. *Langmuir* **1997**, *13*, 3807.
- (36) Pickering, J. P.; Vancso, G. J. *Polym. Bull.* **1998**, *40*, 549.
- (37) Lammertink, R. G. H.; Hempenius, M. A.; Vancso, G. J. *Langmuir* **2000**, *16*, 6245.
- (38) Fasolka, M. J.; Banerjee, P.; Mayes, A. M.; Pickett, G.; Balazs, A. C. *Macromolecules* **2000**, *33*, 5702.
- (39) Harrison, C.; Park, M.; Chaikin, P.; Register, R. A.; Adamson, D. H.; Yao, N. *Macromolecules* **1998**, *31*, 2185.
- (40) (a) Koppi, K. A.; Tirrell, M.; Bates, F. S. *J. Rheol.* **1994**, *38*, 999. (b) Sakurai, S.; Hashimoto, T.; Fetters, L. J. *Macromolecules* **1996**, *29*, 740.
- (41) Seeck, O. H.; Kaendler, I. D.; Tolan, M.; Shin, K.; Rafailovich, M. H.; Sokolov, J.; Kolb, R. *Appl. Phys. Lett.* **2000**, *76*, 2713.
- (42) Parratt, L. G. *Phys. Rev.* **1954**, *95*, 359.
- (43) (a) Kim, G.; Libera, M. *Macromolecules* **1998**, *31*, 2569. (b) Kim, G.; Libera, M. *Macromolecules* **1998**, *31*, 2670.
- (44) Mansky, P.; Chaikin, P.; Thomas, E. L. *J. Mater. Sci.* **1995**, *30*, 1987.

MA000559J